Title

Localization and immobilization of SpoIIQ

Journal

Molecular Microbiology, 89(6)

ISSN

0950-382X

Authors

Fredlund, Jennifer
Broder, Dan
Fleming, Tinya
et al.

Publication Date

2013-09-01

DOI

10.1111/mmi.12333

Peer reviewed

Published in final edited form as:
Mol Microbiol. 2013 September ; 89(6): 1053–1068. doi:10.1111/mmi.12333.

The SpoIIQ landmark protein has different requirements for septal localization and immobilization

Jennifer Fredlund[1,3], **Dan Broder**[1], **Tinya Fleming**, **Clemence Claussin**, and **Kit Pogliano**[2]
Division of Biological Sciences, University of California at San Diego, 9500 Gilman Drive, La Jolla, CA 92093-0377

Summary

Bacillus subtilis sporulation depends on the forespore membrane protein SpoIIQ, which interacts with the mother cell protein SpoIIIAH at the septum to localize other sporulation proteins. It has remained unclear how SpoIIQ localizes. We demonstrate that localization of SpoIIQ is achieved by two pathways: SpoIIIAH and the SpoIID, SpoIIM, SpoIIP engulfment proteins. SpoIIQ shows diffuse localization only in a mutant lacking both pathways. Super-resolution imaging shows that in the absence of SpoIIIAH, SpoIIQ forms fewer, slightly larger foci than in wild type. Surprisingly, photobleaching experiments demonstrate that, although SpoIIQ localizes without SpoIIIAH, it is no longer immobilized, and is therefore able to exchange subunits within a localized pool. SpoIIQ mobility is further increased by the additional absence of the engulfment proteins. However an enzymatically inactive SpoIID protein immobilizes SpoIIQ even in the absence of SpoIIIAH, indicating that complete septal thinning is not required for SpoIIQ localization. This suggests that SpoIIQ interacts with both SpoIIIAH and the engulfment proteins or their peptidoglycan cleavage products. They further demonstrate that apparently normal localization of a protein without a binding partner can mask dramatic alterations in protein mobility. We speculate that SpoIIQ assembles foci along the path defined by engulfment proteins degrading peptidoglycan.

Introduction

A key task in cell biology is to identify factors that contribute to subcellular protein targeting and localization. An amenable system to study this is the sporulation pathway of *Bacillus subtilis*, a developmental program that results in the formation of a durable, dormant endospore and depends on localized proteins. Sporulation commences with the relocalization of cell division proteins from midcell to sites near both cell poles (Levin & Losick, 1996). An asymmetrically positioned division event then creates two adjacent cells of unequal size: a smaller forespore that will ultimately become the spore, and a larger mother cell that lyses after contributing to spore development (reviewed in (Errington, 2003, Piggot & Hilbert, 2004)). Next, the forespore is internalized in a phagocytosis-like process called engulfment, during which the mother cell membrane moves around the forespore until the leading edges of the engulfing membrane meet and fuse, releasing the forespore into the mother cell cytoplasm (Fig. 1A). The resulting forespore is completely enclosed within the mother cell and surrounded by two membranes, one derived from the original forespore membrane and one from the engulfing mother cell membrane. Internalization of the

[2]To whom correspondence should be directed: kpogliano@ucsd.edu. Phone: (858) 822-1314 Mailing address: Natural Sciences Building 4113, 9500 Gilman Drive, La Jolla, CA 92093-0377.
[1]These authors contributed equally to this work.
[3]Current affiliation: Institut Pasteur, Unité ‘Dynamique des interactions hôte-pathogène,’ 25 Rue du Dr. Roux, 75724 Paris, France.

forespore allows subsequent steps in spore maturation, such as coat assembly, to occur in a controlled environment, likely contributing to the extreme durability of the final endospore.

Sporulation critically depends on the localization of proteins involved in morphogenesis and signal transduction to the septum that forms the boundary between the two cells (Shapiro *et al.*, 2009, Driks *et al.*, 1994, Arigoni *et al.*, 1995, Abanes-De Mello *et al.*, 2002, Rubio & Pogliano, 2004). Three pathways for localization to the septum have been identified. First, the SpoIIB protein localizes to potential cell division sites and remains at the septum (Perez *et al.*, 2000), where it acts as a landmark for localization of three mother cell-produced engulfment proteins, SpoIID, SpoIIM and SpoIIP (Fig. 1B) (Aung *et al.*, 2007, Chastanet & Losick, 2007). Second, the SpoVM protein recognizes the convex outer forespore membrane generated during engulfment by directly recognizing the lipid architecture and inserting the non-polar face of its amphipathic helix into the bilayer (Ramamurthi *et al.*, 2009, Prajapati *et al.*, 2000). SpoVM then recruits proteins that assemble the spore cortex and coat to the outer forespore membranes (McKenney & Eichenberger, 2012, Ramamurthi *et al.*, 2006, van Ooij & Losick, 2003, Levin *et al.*, 1993, Driks et al., 1994). Third, the forespore-produced protein SpoIIQ and the mother cell-produced protein SpoIIIAH interact via their extracellular domains within the septal space (Blaylock *et al.*, 2004) (Fig. 1C), tethering both proteins to the septum that is the only potential site of interaction. The SpoIIQ-SpoIIIAH zipper complex subsequently recruits the mother cell membrane proteins required for activation of engulfment-dependent gene expression to foci surrounding the forespore (Jiang *et al.*, 2005, Doan *et al.*, 2005, Doan *et al.*, 2009). The SpoIIQ-SpoIIIAH complex is also required for the complete encasement of the forespore by coat proteins, as in its absence these proteins fail to wrap around the forespore (McKenney & Eichenberger, 2012).

Protein targeting is critical to survival of the developing cell, as *B. subtilis* cells are irreversibly committed to sporulation after the onset of engulfment, so if development fails after this point, the cell will die (Dworkin & Losick, 2005). Thus, it is perhaps not surprising that two of the identified pathways that localize proteins essential for engulfment are redundant to one another. Specifically, while SpoIIB is the primary localization pathway for the SpoIID, SpoIIM and SpoIIP engulfment proteins (Chastanet & Losick, 2007, Aung et al., 2007), the SpoIIQ-SpoIIIAH complex can localize these proteins in the absence of SpoIIB via SpoIVFA, a mother cell protein needed for engulfment-dependent gene expression (Aung et al., 2007). Thus, cell biological evidence suggests that SpoIIQ and SpoIIIAH can localize the SpoIID, SpoIIM and SpoIIP engulfment proteins as well as the two protein complexes that activate engulfment-dependent gene expression (SpoIVFA-SpoIVFB-BofA and SpoIIIAA-AH). This is supported by biochemical data that SpoIIQ and SpoIIIAH form a large complex *in vivo* (Chiba *et al.*, 2007) that includes several of these proteins (Doan et al., 2009) and has been proposed to form a channel (Doan et al., 2009, Meisner *et al.*, 2008, Camp & Losick, 2009). However, it remains unclear if all of these proteins reside in a single large complex or if biochemically distinct complexes exist within the cell.

The SpoIIQ-SpoIIIAH complex also plays a second critical function during engulfment, a process that primarily depends on the SpoIID, SpoIIM and SpoIIP proteins, which are rate limiting for engulfment (Abanes-De Mello *et al.*, 2002, Gutierrez *et al.*, 2010). During this process, SpoIID and SpoIIP degrade peptidoglycan in a coordinated manner, consistent with the model that their processive activity generates force for membrane migration (Abanes-De Mello et al., 2002, Chastanet & Losick, 2007, Morlot *et al.*, 2010, Gutierrez et al., 2010). However, when the activity of SpoIID, SpoIIM or SpoIIP is limited, two processes that are normally not essential for engulfment contribute to membrane migration: peptidoglycan biosynthesis (Meyer *et al.*, 2010) and the SpoIIQ-SpoIIIAH complex (Broder & Pogliano, 2006). The SpoIIQ-SpoIIIAH complex can also mediate engulfment in protoplasts formed

by digestion of the cell wall with lysozyme, and this engulfment does not depend on SpoIID, SpoIIM or SpoIIP (Broder & Pogliano, 2006). Photobleaching experiments have indicated that SpoIIQ is immobile, suggesting that the SpoIIQ-SpoIIIAH complex acts as a stable scaffold, or ratchet, to resist the backward motion of the engulfing mother cell membrane (Broder & Pogliano, 2006). This could ensure that the enzymes that degrade peptidoglycan remain processive in intact cells and allow protoplasts to harness Brownian motion to support forward membrane movement. Interestingly, SpoIIQ regains mobility within the membrane after the completion of engulfment (Chiba et al., 2007), suggesting that it might be present in a different protein complex after, versus during, engulfment.

Curiously, although SpoIIIAH localization depends on SpoIIQ, SpoIIQ remains localized in the absence of SpoIIIAH, forming foci and helical arcs that look nearly identical to those assembled in wild type cells (Blaylock et al., 2004, Jiang *et al.*, 2005). However, the absence of the mother cell specific sigma factor σ^E completely delocalizes SpoIIQ (Rubio & Pogliano, 2004), suggesting that other mother cell produced proteins are responsible for SpoIIQ localization (Fig. 1D). We here demonstrate that septal localization of SpoIIQ is mediated by two redundant systems, SpoIIIAH and the SpoIID, SpoIIM, SpoIIP engulfment proteins, either of which can retain SpoIIQ at the septum in the absence of the other. We also observed that although SpoIIQ forms foci in the absence of SpoIIIAH, it is no longer immobilized and shows localized diffusion within the septum that forms the interface between the forespore and mother cell. The additional absence of SpoIID, SpoIIM, and SpoIIP allows SpoIIQ to be released from the septum where it diffuses even more rapidly, suggesting that the SpoIID, SpoIIM, and SpoIIP engulfment proteins form a secondary tether to localize SpoIIQ to the sporulation septum. Using mutations that abolish SpoIID peptidoglycan degradation activity, we also show that SpoIIQ is immobilized even in the absence of SpoIIIAH if the SpoIID/SpoIIM/SpoIIP complex is itself trapped at the septum. These findings demonstrate an intimate interaction between the SpoIID, SpoIIM and SpoIIP engulfment proteins or the peptidoglycan products of their activity and the SpoIIQ-SpoIIIAH complex, which is required for engulfment-dependent gene expression.

Results

Localization of GFP-SpoIIQ depends on both SpoIIIAH and SpoIIDMP

Deconvolution microscopy revealed that localization of GFP-SpoIIQ is not dramatically affected by the removal of its only known mother cell tether, SpoIIIAH ((Blaylock et al., 2004, Jiang et al., 2005) Fig. 2A, F), although elimination of all mother cell specific gene expression by a *spoIIGB* mutation completely delocalizes GFP-SpoIIQ (Rubio & Pogliano, 2004). We therefore sought to identify members of the σ^E regulon required for SpoIIQ localization. SpoIIQ and SpoIIIAH play an auxiliary role in engulfment, and disruption of *spoIIQ* in strains expressing low levels of SpoIID or SpoIIP, or expressing GFP fusions to SpoIID, SpoIIM, or SpoIIP (which complement their respective nulls for spore formation), produces synergistic engulfment defects (Broder & Pogliano, 2006). This suggests that these two protein complexes might interact. We therefore examined the role of the engulfment proteins, SpoIID, SpoIIM, and SpoIIP, in localization of GFP-SpoIIQ.

Disruption of *spoIID*, *spoIIM*, or *spoIIP* prevents membrane migration and formation of GFP-SpoIIQ foci and arcs, but GFP-SpoIIQ is still retained at the septum (Fig 2B-D). Quantification revealed that GFP-SpoIIQ localized to the septum in most (74-92%) *spoIID*, *spoIIM*, or *spoIIP* single mutant sporangia, forming a bright focus at the center or two foci on either side of the bulges (Fig. 2B-D, M). Three GFP-SpoIIQ localization phenotypes were observed in the *spoIID, spoIIM, spoIIP* triple mutant: 46% of sporangia showed septal localization, 20% showed a uniform distribution throughout the forespore membrane and 34% showed an intermediate localization phenotype (Fig. 2E, M). In contrast, GFP-SpoIIQ

localizes exclusively to the septum in >98% of all wild type sporangia at early stages of engulfment (Fig. 2A; quantified in (Rubio & Pogliano, 2004)). The variable and intermediate phenotype seen in the mutant background might indicate that GFP-SpoIIQ localization is delayed in the absence of the engulfment proteins, but testing localization at later timepoints is not possible because engulfment defective mutants ultimately lyse. However, because SpoIIQ is expressed only after polar septation (Londono-Vallejo *et al.*, 1997), we can use GFP-SpoIIQ fluorescence intensity as a proxy for time after initial expression, since cells with more GFP fluorescence have been expressing SpoIIQ for longer times. Thus, if the variable SpoIIQ localization in the absence of all three engulfment proteins represents a kinetic defect in localization, we would expect less localization in cells with low GFP intensity (early) and more localization in cells with higher GFP intensity (late). Contrary to this prediction, delocalized GFP-SpoIIQ was seen in both early (dim) and later (bright) cells, as was localized GFP-SpoIIQ (Figure 2E). Thus the variable localization in this strain is unlikely to be due to a kinetic defect in SpoIIQ localization, but is more likely to reflect cell to cell variation in localization. This suggests that although SpoIID, SpoIIM, and SpoIIP contribute to SpoIIQ localization, another protein also can mediate SpoIIQ localization.

We next tested if SpoIIQ localization in the absence of the SpoIID, SpoIIM, and SpoIIP engulfment proteins depended on its mother cell binding partner SpoIIIAH by inactivating *spoIIIAH* in the single and triple engulfment mutants. While all three single engulfment gene null mutant/*spoIIIAH* mutant combinations resulted in a variety of GFP-SpoIIQ localization phenotypes, the *spoIID spoIIIAH* strain retained significantly more localization than the other strains (Fig. 2I, M), with the most frequent pattern being a focus at the septum center (32%). This was never observed in *spoIIP spoIIIAH* or *spoIIM spoIIIAH* (Fig. 2G-H, M) strains, which showed either partial or completely delocalized GFP-SpoIIQ. These data suggest that multiple engulfment proteins contribute to localizing SpoIIQ to the septum (Fig. 2D, J), directly or indirectly, but not necessarily to the same extent. Combination of all three engulfment mutant alleles with the *spoIIIAH* mutation resulted in random localization identical to the σ^E null strain in 93% of sporangia (Fig. 2F, J). These results, which were verified by using immunofluorescence microscopy to localize native SpoIIQ (Fig. S1), indicate that the SpoIID/SpoIIM/SpoIIP complex and SpoIIIAH each contribute, directly or indirectly to SpoIIQ localization. A similar result was also obtained by D. Rudner and colleagues (Rodriguez *et al*, 2013).

SpoIIIAH is required to immobilize GFP-SpoIIQ

When expressed at native levels, GFP-SpoIIQ is immobile during engulfment ((Broder & Pogliano, 2006); confirmed in Fig 3A), but the mechanism for immobilization remains unclear. We therefore sought to determine which of the above localization determinants were responsible for immobilization of SpoIIQ by performing a Fluorescence Recovery After Photobleaching (FRAP) analysis on GFP-SpoIIQ in mutants lacking SpoIIIAH and/or the engulfment proteins. Sporulating cells were immobilized on coverslips and a region of the GFP-SpoIIQ fluorescence was photobleached in engulfing cells. The bleached region corresponded to a single focus or to half of the septum depending on the GFP-SpoIIQ localization pattern and extent of engulfment. Recovery of the bleached region was then observed using timelapse fluorescence microscopy and the images quantified using two different methods. First, to obtain individual cell recovery curves, the “edit polygon” tool of SoftWRX software was used to draw polygons defining the entire bleached and unbleached regions of each forespore. The amount of fluorescence per pixel was then determined for each region in each image of the timelapse sequence with a correction for background signal (as described in (Broder & Pogliano, 2006)). Bacterial cells are small relative to the size of the bleached region, so there is a limited pool of unbleached GFP for recovery, so

fluorescence recovery is accompanied by loss of fluorescence in the unbleached region. Complete recovery is defined by the two plots converging on the pixel intensity expected following equilibration between the bleached and unbleached regions. Second, to obtain average recovery curves of many cells, we calculated the ratio of fluorescence intensity of the bleached region to that of the unbleached region at each timepoint relative to the ratio of the same regions before the bleach to give the corrected recovery index (cRI; (Wu *et al.*, 2006)). Recovery curves were then normalized by defining the initial prebleach cRI value as one and the minimum cRI ratio (immediately after photobleaching) as zero to give the corrected fraction recovery (cFR; as in (Fleming *et al.*, 2010), adapted from (Wu et al., 2006)). Note that we are bleaching a relatively large area of a small cell, so that after complete equilibration between the bleached and unbleached regions, the cFR will be less than 1.0 since photobleaching affects a significant fraction of the pool of fluorescent protein. The average recovery after complete equilibration was observed to be 0.7, suggesting that on average, we bleached 30% of the available GFP-SpoIIQ. We then averaged the data at each timepoint and performed a curve fit analysis of each bleach event and of the average (see Materials and Methods). From the curve fits, we obtained the average time to 50% recovery ($t_{1/2}$ avg) relative to the maximum recovery ($t_{1/2}$ avg = cFR of 0.35) and the average mobile fraction, or amount of protein able to move within the septum, which is represented by the maximum recovery in the cFR.

In wild type cells, GFP-SpoIIQ showed little recovery after photobleaching in engulfing cells, even in experiments lasting up to 5 minutes, with an average cFR of 0.2 (20%) versus the ∼0.7 (70%) expected for a fully mobile protein when 30% of the pool is lost in the bleach event (Fig 3A). This indicates that that there is little or no movement of SpoIIQ between the bleached and unbleached regions and that the protein is immobile as previously described (Broder & Pogliano, 2006). GFP-SpoIIQ appears normally localized in the *spoIIIAH* mutant (Fig. 2F; (Blaylock et al., 2004)), so we expected it would be immobile as in the wild type strain. In contrast, the protein rapidly recovered to 70% the level of prebleach fluorescence, with an average equilibration half time ($t_{1/2}$) of approximately 19 seconds (Fig. 3B, K). Strikingly, in many sporangia, GFP-SpoIIQ assembled clear foci and the bleaching of individual foci often resulted in recovery of fluorescence in the same focus as it appeared before photobleaching. Thus, although SpoIIQ appears normally localized in the absence of SpoIIIAH, it displays dramatically increased mobility, indicating that the zipper-like interaction between SpoIIQ and SpoIIIAH immobilizes SpoIIQ.

SpoIIQ assembles a structure including additional membrane proteins encoded by the entire *spoIIIA* operon (Doan et al., 2009, Meisner et al., 2008, Camp & Losick, 2009). We therefore tested the possibility that other members of the *spoIIIA* operon affect GFP-SpoIIQ mobility. To do so, we examined the effect of a *spoIIIAA::mTn5* mutation that prevents expression of all the genes in the *spoIIIAA-AF* operon, but does not affect expression of the *spoIIIAG-H* operon (Blaylock et al., 2004). This mutation had no effect on GFP-SpoIIQ mobility (data not shown). We attempted to specifically deplete SpoIIIAH, but mutations in *spoIIIAH* destabilized SpoIIIAG (Chiba et al., 2007), so we were unable to determine if both SpoIIIAG and SpoIIIAH are required for SpoIIQ immobilization. Thus, it remains possible that SpoIIIAG participates in the interaction with SpoIIQ, but for simplicity we will here use the model in which SpoIIQ immobilization primarily depends on SpoIIIAH, with which it interacts robustly (Blaylock et al., 2004, Doan *et al.*, 2005).

We next tested if the engulfment proteins are necessary for immobilization of SpoIIQ. FRAP experiments demonstrated that GFP-SpoIIQ showed limited mobility in the *spoIID, spoIIM, spoIIP* triple mutant, with the equilibration half times for most cells longer than the experiment duration of 3 or 5 minutes and with limited recovery similar to the mobility of the protein in wild type cells. Thus, despite the observation that SpoIIQ fails to localize in

17% of sporangia lacking the engulfment proteins, it remains immobilized in this strain (Fig. 3C). Recovery was also very slow in the single engulfment mutants (data not shown) within which GFP-SpoIIQ predominantly localizes as a focus at the septum middle. This indicates that immobilization of SpoIIQ does not depend on the engulfment proteins.

Although GFP-SpoIIQ mobility was increased by the absence of SpoIIIAH, its $t_{1/2}$ (18.9 +/- 10.2 sec) was significantly longer than previously demonstrated for a forespore expressed membrane protein that is not expected to specifically interact with other proteins, MalF-GFP (4 sec, (Rubio & Pogliano, 2004, Broder & Pogliano, 2006)). We therefore speculated that, in the absence of SpoIIIAH, GFP-SpoIIQ mobility was restricted by its interaction with other proteins. The engulfment proteins were likely candidates, since GFP-SpoIIQ does not localize in the *spoIID, spoIIM, spoIIP, spoIIIAH* quadruple mutant strain. Indeed, FRAP experiments showed that in this strain, GFP-SpoIIQ showed very rapid and nearly complete fluorescence recovery after photobleaching (Fig. 3D) with a $t_{1/2}$ reduced to 2.4 +/- 1.3 sec (Fig. 3K) and recovery >60% (Fig. 3J), similar to that of forespore expressed MalF-GFP (Broder & Pogliano, 2006)). This suggests that we have identified and eliminated all proteins that influence SpoIIQ mobility in the forespore.

SpoIID, SpoIIM, and SpoIIP affect SpoIIQ mobility differently

To further elucidate the individual contributions of the engulfment proteins in SpoIIQ immobilization, we used FRAP to examine GFP-SpoIIQ mobility in mutants lacking SpoIIIAH and either SpoIID, SpoIIM or SpoIIP. Interestingly, combining the *spoIIIAH* deletion with the *spoIID, spoIIM* and *spoIIP* single null mutants produced a wide range of outcomes (Fig. 3E-G) compared to the *spoIID, spoIIM, spoIIP, spoIIIAH* quadruple mutant that showed a fairly uniform recovery (Fig. 3D). For example, FRAP of the *spoIIP spoIIIAH* double mutant revealed some cells that either (1) recovered more rapidly than a *spoIIIAH* mutant or (2) did not recover at all, with curves mimicking those of wild type. Thus, some *spoIIP spoIIIAH* cells had a fraction of SpoIIQ that was rapidly diffusing, while others showed fully immobilized SpoIIQ. The *spoIID spoIIIAH* and *spoIIM spoIIIAH* double mutants also showed mixed populations. Plotting the time at which individual cells reached the ½ maximal cFR for SpoIIQ (0.7) more clearly shows populations of cells that were either immobilized similar to wild type or mobile to an extent similar to the *spoIIIAH* null or the *spoIID, spoIIM, spoIIP, spoIIIAH* quadruple mutant (Fig. 3K). There was no apparent correlation between the degree of localization and the rate of diffusion: SpoIIQ with similar localization patterns could be either mobile or immobile (Fig. S2). Thus, in these strains, sporangia that were completely delocalized could show either rapidly diffusing or immobile SpoIIQ. These results indicate that, in the absence of SpoIIIAH and either SpoIID, SpoIIM or SpoIIP, the mobility of SpoIIQ is restricted by interactions with one or more of the remaining engulfment proteins or the peptidoglycan cleavage products they produce. They also suggest that, in the absence of SpoIIIAH, an intact SpoIID, SpoIIM, SpoIIP complex is required to stabilize the interaction of SpoIIQ with its secondary tether.

Mutations that abolish the enzymatic activity of SpoIID enzymatic mutants affect SpoIIQ mobility

Our results suggest that SpoIIQ either interacts directly with the engulfment proteins or their peptidoglycan cleavage products, or that the thick peptidoglycan that accumulates at the septal midpoint in the absence of the engulfment proteins inhibits the interaction of SpoIIQ with another unidentified mother cell protein that comprises its secondary tether. To discriminate between these models, we made use of a recently identified mutant of SpoIID that localizes to the septum but is unable to cleave peptidoglycan, $SpoIID^{E88A}$ (Gutierrez et al., 2010), and fails to support septal thinning or membrane migration. If thick or incompletely digested septal peptidoglycan prevents the interaction of SpoIIQ with its bona

fide secondary tether in the mother cell, then this mutant should behave in a manner similar to the *spoIID* null mutation, showing a mixture of mobile and immobile protein in the *spoIIIAH* background. However, this mutant differs from the null as it is capable of moving SpoIIP across the septum, likely allowing SpoIIP to produce denuded glycan chains across the septal disk, whereas in the *spoIID* null mutant, SpoIIP remains trapped at the septal midpoint limiting production of denuded glycan chains (Gutierrez et al., 2010). Importantly, *in vitro* SpoIIP makes the same denuded peptidoglycan chains without SpoIID as it does with the SpoIID^{E88A} mutant protein (Morlot, et al, 2010). If SpoIIQ interacts directly with the engulfment proteins or with the denuded glycan chains produced by SpoIIP, then we expect different outcomes in these two strains, and SpoIID^{E88A} might trap SpoIIQ at the septum even in the absence of SpoIIIAH.

When the SpoIID^{E88A} protein was expressed in an otherwise wild type GFP-SpoIIQ strain, we found no effect on SpoIIQ mobility, and no recovery was seen within 3 minutes (data not shown). However, when combined with a *spoIIIAH* deletion, SpoIID^{E88A} showed improved GFP-SpoIIQ localization (Fig. 2K) compared to the *spoIID* null mutant (Fig. 2I). The mutation also dramatically reduced the mobility of SpoIIQ compared to either the *spoIIIAH* single mutant strain or the *spoIID spoIIIAH* strain, with 20 of the 22 cells tested showing no recovery in FRAP experiments (Fig. 3H, J, K). Thus, the enzymatically inactive mutant of SpoIID reduces SpoIIQ mobility in the absence of SpoIIIAH, whereas the complete absence of SpoIID protein in the null mutant strain increases SpoIIQ mobility in the absence of SpoIIIAH. This is not consistent with the model that septal peptidoglycan reduces the ability of SpoIIQ to interact with another mother cell binding protein, and instead supports the model that SpoIIQ directly interacts with two or more members of the SpoIID, SpoIIM and SpoIIP complex or their peptidoglycan cleavage products. Interestingly, we had previously demonstrated that this enzymatically inactive mutant effectively locks down SpoIID at the septum (Gutierrez et al., 2010), and our present results suggest that it also traps SpoIIQ in an immobile complex in the absence of SpoIIIAH.

Immobilization of GFP-SpoIIIAH requires SpoIIQ

Previous results indicated that SpoIIIAH localizes in a manner similar to SpoIIQ, being enriched around the forespore and co-localizing with SpoIIQ (Blaylock et al., 2004, Doan et al., 2005). We were interested in determining if SpoIIIAH was immobilized by interaction with SpoIIQ, and therefore constructed a GFP fusion to the N-terminus of SpoIIIAH. GFP-SpoIIIAH produced foci associated with the forespore membrane (Fig. 4A). The *spoIIQ* mutation resulted in decreased, though not completely random, SpoIIIAH localization, with increased signal in the mother cell cytoplasm and membrane as previously reported (Blaylock et al., 2004, Doan et al., 2005). This confirms that SpoIIQ is the primary localization determinant of SpoIIIAH (Fig. 4B). Removal of either one or all three essential engulfment proteins, SpoIID, SpoIIM, and SpoIIP, had no effect on GFP-SpoIIIAH localization and the protein localized both to the septum and to the septal bulges produced in these mutants (Fig. 4C-F). This is in contrast to a previous localization of epitope-tagged SpoIIIAH by immunofluorescence microscopy, which showed an early localization defect in the absence of the engulfment proteins (Blaylock et al., 2004). We found no evidence for this defect, and suggest that the difference is either due to differences in the epitope tag or to the requirement to permeabilize the cells using lysozyme during immunofluorescence. These results again suggest that septal peptidoglycan does not provide a barrier for the interaction between SpoIIIAH and SpoIIQ. Furthermore, the elimination of all three engulfment proteins did not reduce septal localization of SpoIIIAH in the absence of SpoIIQ (Fig. 4B, G), suggesting that they do not contribute to the apparent residual targeting of SpoIIIAH in the absence of SpoIIQ. Indeed, this apparent residual septal localization might simply be due

to the lack of engulfment and, therefore, formation of septa that have extra membrane, as indicated by the increased staining with Mitotracker Red.

Based on observations of GFP-SpoIIQ dynamics during FRAP experiments, we hypothesized that GFP-SpoIIIAH would also be immobilized in a manner that depends on its partner SpoIIQ. Indeed, photobleaching of GFP-SpoIIIAH resulted in very limited recovery similar to that of GFP-SpoIIQ (Fig. 5A). A similar phenomenon was observed in the *spoIIP* strain (Fig. 5B). In contrast, the absence of SpoIIQ allowed rapid and nearly complete recovery of photobleached GFP-SpoIIIAH to a cFR =0.8 and recovery $t_{1/2}$ of ∼25 seconds (Fig. 5C, D). Curiously, this recovery was not as fast as that of GFP-SpoIIQ in the absence of SpoIIIAH, suggesting that diffusion of SpoIIIAH is further restricted by some other interaction, perhaps with SpoIIIAG, or with proteins encoded by the *spoIVFA-FB* and *spoIIIAA-AF* operons, which interact with SpoIIIAH and localize to the septum in a SpoIIIAH-dependent manner (Blaylock et al., 2004, Doan et al., 2005, Jiang et al., 2005). Further studies are required to determine if any of these proteins interact with SpoIIIAH in the absence of SpoIIQ. Together, our FRAP data indicate that the interaction between SpoIIQ and SpoIIIAH immobilizes both proteins.

Super-resolution imaging shows subtle differences in GFP-SpoIIQ localization in the absence of SpoIIIAH

The SpoIIQ-SpoIIIAH complex assembles foci surrounding the forespore, but the limited resolution of fluorescence microscopy has made it unclear if these foci form a specific structure around the forespore, such as a helix. To further investigate SpoIIQ architecture and to determine if the absence of SpoIIIAH produced subtle changes in SpoIIQ structure, we localized GFP-SpoIIQ in the presence and absence of SpoIIIAH using structured illumination microscopy to achieve ∼100 nm lateral resolution. In the wild type strain GFP-SpoIIQ localized to discrete foci surrounding the forespore after the onset of engulfment (Fig. 6A, arrows). Reconstruction of the optical stacks and rotation of the resulting image revealed that SpoIIQ assembles a fairly disordered assortment of foci and short arcs that formed a single cup during early stages of engulfment, and two hemispheres later in engulfment (Fig. 6C). However, prior to engulfment GFP-SpoIIQ appeared to be more distributed throughout the forespore membrane than previously indicated by epifluorescence microscopy, which has lower spatial resolution. In contrast, in the *spoIIIAH* mutant, SpoIIQ foci appeared somewhat larger and less discrete (Fig. 6B, arrowheads). To quantify this subtle difference, we calculated the area of each foci and the number of foci per cell (Table 1). This analysis revealed that the absence of SpoIIIAH led to a significantly increased average focus size, from 0.032 μm^2 in wild type to 0.044 μm^2 in *spoIIIAH* ($P = 0.02$) and a decrease in the number of foci per cell, from 1.96 to 1.55 ($p= 0.0018$). The two strains show a different distribution of GFP-SpoIIQ focus sizes, with the wild type showing a more narrow size range than the *spoIIIAH* strain, as is also reflected in the larger standard deviation in the *spoIIIAH* strain (Fig. 6D and Table 1). Thus, the absence of SpoIIIAH causes subtle changes in SpoIIQ architecture visible only with super-resolution imaging. The larger and fewer SpoIIQ foci in a *spoIIIAH* background are consistent with the alterations in localization likely to result from increased SpoIIQ mobility and might reflect the DMP-dependent SpoIIQ localization pattern.

Discussion

We here demonstrate that the interaction between the forespore protein SpoIIQ and the mother cell protein SpoIIIAH immobilizes both proteins during engulfment. This immobilization is consistent with the ability of this protein complex, which spans the two cells of the sporangium, to facilitate engulfment by preventing backwards movement of the

migrating membrane (Broder & Pogliano, 2006). Interestingly, although immobilization of each protein depends on the other (Fig. 3, 5), the septal localization of just one of these proteins, SpoIIIAH, depends on the other, since SpoIIQ remains localized in the absence of SpoIIIAH (Blaylock et al., 2004, Rubio & Pogliano, 2004). However, our FRAP results demonstrate that despite continued localization of SpoIIQ in the absence of SpoIIIAH, SpoIIQ itself shows increased dynamics, with individual subunits moving between different foci within the cell. Thus, the SpoIIQ-SpoIIIAH complex that spans the two cells of the developing sporangium also immobilizes both protein components, perhaps because the large complex becomes embedded in peptidoglycan that is synthesized during engulfment (Meyer et al., 2010).

We further demonstrated that in the absence of SpoIIIAH, SpoIIQ diffuses between these foci more slowly than expected for an unfettered membrane protein (Rubio & Pogliano, 2004, Broder & Pogliano, 2006), suggesting that it has at least one other interaction that slows its diffusion in the absence of SpoIIIAH (Fig. 2). Indeed, when we eliminated all three engulfment proteins, SpoIID, SpoIIM, and SpoIIP, in conjunction with SpoIIIAH, SpoIIQ failed to localize (Fig. 2) and its mobility increased to match that of a freely diffusing membrane protein (<5 sec (Rubio & Pogliano, 2004)) (Fig. 3). This suggests that in the absence of SpoIIIAH, SpoIIQ mobility is slowed by an interaction that depends on one or more of the engulfment proteins or their peptidoglycan cleavage products. These data indicate that septal localization of the forespore-expressed SpoIIQ protein can be mediated by its interaction with either one of two mother cell tethers: the SpoIIIAH protein or a second tether that requires the SpoIID/SpoIIM/SpoIIP complex of engulfment proteins. This second tether could either be the engulfment proteins themselves, or it could be the peptidoglycan cleavage products they generate. However, if the secondary tether was only comprised of peptidoglycan cleavage products, then eliminating SpoIIP should eliminate the tether since SpoIIP initiates peptidoglycan degradation (Morlot et al., 2010), whereas all three proteins must be absent to significantly delocalize SpoIIQ experimentally. Interestingly, the FRAP recovery curves for the *spoIIM spoIIIAH, spoIID spoIIIAH* and *spoIIP spoIIIAH* double mutant strains each show variable SpoIIQ mobility, while the absence of all three engulfment proteins and SpoIIIAH produces uniformly mobile SpoIIQ. We therefore favor the hypothesis that the secondary tether is comprised of several weak interactions with the SpoIID/SpoIIM/SpoIIP complex and the modified peptidoglycan it produces.

In support of this, if SpoIID is enzymatically inactive and unable to be released from the septum (Gutierrez et al., 2010), then SpoIIQ is immobilized even in the absence of SpoIIIAH. This indicates not only that this mutant traps SpoIID at the septum, but that it also traps SpoIIQ, and suggests a complex is formed between SpoIIQ and one or more of the engulfment proteins or peptidoglycan, although we cannot completely rule out the possibility that SpoIIQ interacts with another protein trapped at the septum in this mutant. Additionally, biochemical studies indicate that SpoIIP can cleave peptidoglycan without SpoIID (Morlot et al., 2010) although *in vivo*, SpoIID is required to move SpoIIP across the septum (Aung *et al.*, 2007; Gutierrez et al., 2010). The enzymatically inactive SpoIID mutant retains this functionality, so it is likely that in the SpoIID^{E88A} strain, SpoIIP remains enzymatically active and cleaves peptidoglycan as it moves across the septum. If so, then SpoIIQ might also bind to the denuded glycan chains generated by SpoIIP cleavage, in addition to interacting with one or more of the engulfment proteins.

Based on these findings, we propose a model whereby newly synthesized SpoIIQ is inserted into the forespore membrane where it weakly and transiently interacts with the engulfment protein complex, SpoIID, SpoIIM and SpoIIP, or the peptidoglycan intermediates created during peptidoglycan degradation or synthesis (Fig. 7). This mechanism could be similar to

current models for clathrin-coated pit formation in eukaryotes, which involve a series of weak interactions between phosphoinositides, AP-2 and clathrin that lead to stochastic initiation of complex assembly and subsequent stabilization through continued binding of AP2, clathrin and other adaptors and eventually pit formation after the higher affinity interaction of cargo binding (Cocucci *et al.*, 2012, Swan, 2013). In our system, the initial, low-affinity interactions would create a high concentration of SpoIIQ in the septum, near the SpoIIDMP complex, thereby facilitating binding with SpoIIIAH. This interaction generates an immobile complex, with little or no cycling of SpoIIQ or SpoIIIAH in or out of the complex, and little or no diffusion of the complex within the membrane. Hence, we speculate that the large SpoIIQ/SpoIIIAH complex predicted to form in the intermembrane space (Camp & Losick, 2009, Camp & Losick, 2008, Meisner *et al.*, 2008) could be held in place by septal peptidoglycan that either remains after septal thinning or is synthesized during engulfment (Meyer et al., 2010). Consistent with this hypothesis, we have recently used cryoelectron tomography to demonstrate that peptidoglycan remains in the septum throughout early stages of engulfment (Tocheva *et al.*, 2013). Interestingly, SpoIIQ foci and arcs depend on the engulfment proteins rather than on SpoIIIAH. We therefore speculate that the pattern of SpoIIQ deposition and localization corresponds to the path taken by the engulfment protein complex as it moves around the forespore during membrane migration.

Experimental Procedures

Strains, genetic manipulations and growth conditions

Strains (Table 2) are derivatives of *B. subtilis* PY79 (Youngman *et al.*, 1984). Mutations were introduced by transformation (Dubnau & Davidoff-Abelson, 1971). Sporulation was induced by resuspension (Sterlini & Mandelstam, 1969) at 37°C with the modification that initial growth was performed using 0.25× LB in most cases. When used, CH medium was prepared using casein hydrolysate from EMD, due to variability in the ability of Oxoid brand casein hydrolysate to support sporulation.

Genetic constructions

An N-terminal GFP fusion to SpoIIIAH expressed from the *spoIIIAA* promoter was created as follows. A 600 bp fragment encoding the *spoIIIAA* promoter was amplified via PCR with Pfu polymerase using oligonucleotides DB121 (5′-ACTGAAAGGATCCGGGCTTGTTGTAAACGTGCCG-3′) and DB209 (5′-TTT ATC ATT ACT AGT TTG TTT TTT AAG CAT CAG AGC CTC CTC CTT TCT ACC G-3′), digested with BamHI and SpeI, and ligated into BamHI/SpeI-digested pMDS14 (Sharp & Pogliano, 2002) to create plasmid pDB141. The 654 bp *spoIIIAH* gene was then amplified using oligonucleotides DB177 (5′-GGAGGATGGGCCCATGCTTAAAAAACAAACCG-3′) and DB178 (5′-TCCCTCATTCGGGCCCTTATTTAGAGGGTTC-3′), digested with PspOMI, and ligated into EagI-digested pDB141 to create plasmid pDB142. DNA sequencing was performed by Eton Bioscience Inc. (San Diego, CA). This construct was expressed in a strain expressing the wildtype *spoIIIAG-H* operon because the GFP-SpoIIIAH did not fully complement the null mutant. The various *spoIID* mutants were inserted at the *thrC* locus by subcloning out of pKP01 or PCR products from the amyE locus of strains KP1102 and KP1072 (Gutierrez et al., 2010). SpoIID constructs were digested using enzymes BamHI and SfoI and inserted into pDG1664 (Guerout-Fleury *et al.*, 1996) digested with BamHI and SnaBI, eliminating the erm^R cassette on the plasmid. All plasmids were initially transformed into PY79 and verified to be kan^R, erm^S, spc^S to ensure proper integration of the plasmid at the *thrC* locus. These mutants were combined with a *spoIIIAH* knockout generated from pDB102. pDB102 is pMutinFLAG with a KpnI/HindIII-digested PCR product created with primers DB163 and

DB164 cloned in. When campbelled in, this interrupts the *spoIIIA* operon after *spoIIIAG*, creating a *spoIIIAH* null.

Microscopy, deconvolution, image analysis, and Fluorescence Recovery After Photobleaching (FRAP)

Imaging of FM 4-64 stained cells was performed as described (Rubio & Pogliano, 2004), using an Applied Precision Spectris microscope equipped with a Quantified Laser Module (described in (Liu *et al.*, 2006)). Image files were deconvolved using SoftWoRx (15 iterations on conservative setting). TIFFs were saved from medial focal planes, adjusting the GFP images to eliminate background fluorescence in vegetative cells that do not express GFP, and the FM 4-64 images to eliminate fluorescence outside the cells. Photobleaching experiments to assess GFP-SpoIIQ or GFP-SpoIIIAH mobility used cells from $t_{2.5}$ or t_3 of sporulation that were concentrated, stained with FM 4-64 and applied to poly-$_L$-lysine treated coverslips. Prebleach images were collected for both FM 4-64 and GFP. Photobleaching was achieved using a 0.05 sec pulse of a 488 nm argon laser at 50% power or a 0.3 second pulse at 30% power, and subsequent GFP images were collected at appropriate intervals for either 30, 82, 125, 180 or 300 seconds, depending on the observed recovery time of the GFP fusion. Three sec exposure times were used for GFP-SpoIIIAH, 0.5 sec for GFP-SpoIIQ. Quantification of FRAP experiments was performed as described (Fleming et al., 2010) using the equation $y=A(1-e^{(-Tt)})$ or $y=A(1-e^{(-t/t1)})(Y_0 + B*e^{(-t/t2)})$ for very rapidly recovering curves. Curve fits were discarded if the generated R value was below 0.7. Control experiments demonstrated that identical mobility was observed on timelapse pads (Becker & Pogliano, 2007), which are made without poly-$_L$-lysine.

High-resolution fluorescence microscopy

Samples were prepared as described for epifluorescence microscopy and imaged with the DeltaVision OMX structured illumination microscopy system at UCSD School of Medicine Light Microscopy Facility. Image stacks were acquired with a 100× 1.4 NA Olympus objective, 488nm laser, and EM-CCD camera with z-stack intervals of 0.125nm. These images were deconvolved and aligned using SoftWoRx software to achieve an X-Y resolution of 100nm and Z resolution of 250nm.

Quantification of GFP-SpoIIQ foci number and size

The single optical section with the clearest outline of FM4-64 membrane staining was selected for analysis as representative of the middle of each cell. The ‘threshold’ function of Image J was used to identify pixels with intensity values comprising the top 60% for each cell. These were the only pixels used for analysis to reduce background effects. The number of foci per cell were counted and the area of each foci measured using the ‘analyze particles’ function of ImageJ. The minimum area was set at 0.005 μm^2 (3 square pixels), smaller regions defined by the software were not used.

Supplementary Material

Refer to Web version on PubMed Central for supplementary material.

Acknowledgments

This research was supported by the National Institutes of Health (R01-GM57045). The content is solely the responsibility of the authors and doesn't necessarily represent the official views of the National Institute of Health or the National Institute of General Medical Sciences. The Applied Precision OMX microscope is supported by the UCSD Neuroscience Core, Grant P30 NS04710. We thank Jennifer Santini for technical assistance.

References

Abanes-De Mello A, Sun YL, Aung S, Pogliano K. A cytoskeleton-like role for the bacterial cell wall during engulfment of the *Bacillus subtilis* forespore. Genes Dev. 2002; 16:3253–3264. [PubMed: 12502745]

Arigoni F, Pogliano K, Webb CD, Stragier P, Losick R. Localization of protein implicated in establishment of cell type to sites of asymmetric division [see comments]. Science. 1995; 270:637–640. [PubMed: 7570022]

Aung S, Shum J, Abanes-De Mello A, Broder DH, Fredlund-Gutierrez J, Chiba S, Pogliano K. Dual localization pathways for the engulfment proteins during *Bacillus subtilis* sporulation. Mol Microbiol. 2007; 65:1534–1546. [PubMed: 17824930]

Becker EC, Pogliano K. Cell-specific SpoIIIE assembly and DNA translocation polarity are dictated by chromosome orientation. Mol Microbiol. 2007; 66:1066–1079. [PubMed: 18001347]

Blaylock B, Jiang X, Rubio A, Moran CP Jr, Pogliano K. Zipper-like interaction between proteins in adjacent daughter cells mediates protein localization. Genes Dev. 2004; 18:2916–2928. [PubMed: 15574594]

Broder DH, Pogliano K. Forespore engulfment mediated by a ratchet-like mechanism. Cell. 2006; 126:917–928. [PubMed: 16959571]

Camp AH, Losick R. A novel pathway of intercellular signalling in Bacillus subtilis involves a protein with similarity to a component of type III secretion channels. Mol Microbiol. 2008; 69:402–417. [PubMed: 18485064]

Camp AH, Losick R. A feeding tube model for activation of a cell-specific transcription factor during sporulation in Bacillus subtilis. Genes Dev. 2009; 23:1014–1024. [PubMed: 19390092]

Chastanet A, Losick R. Engulfment during sporulation in Bacillus subtilis is governed by a multi-protein complex containing tandemly acting autolysins. Mol Microbiol. 2007; 64:139–152. [PubMed: 17376078]

Chiba S, Coleman K, Pogliano K. Impact of membrane fusion and proteolysis on SpoIIQ dynamics and interaction with SpoIIIAH. J Biol Chem. 2007; 282:2576–2586. [PubMed: 17121846]

Cocucci E, Aguet F, Boulant S, Kirchhausen T. The first five seconds in the life of a clathrin-coated pit. Cell. 2012; 150:495–507. [PubMed: 22863004]

Doan T, Marquis KA, Rudner DZ. Subcellular localization of a sporulation membrane protein is achieved through a network of interactions along and across the septum. Mol Microbiol. 2005; 55:1767–1781. [PubMed: 15752199]

Doan T, Morlot C, Meisner J, Serrano M, Henriques AO, Moran CP Jr, Rudner DZ. Novel secretion apparatus maintains spore integrity and developmental gene expression in Bacillus subtilis. PLoS Genet. 2009; 5:e1000566. [PubMed: 19609349]

Driks A, Roels S, Beall B, Moran CP Jr, Losick R. Subcellular localization of proteins involved in the assembly of the spore coat of Bacillus subtilis. Genes Dev. 1994; 8:234–244. [PubMed: 8299942]

Dubnau D, Davidoff-Abelson R. Fate of transforming DNA following uptake by competent Bacillus subtilis. I. Formation and properties of the donor-recipient complex. J Mol Biol. 1971; 56:209–221. [PubMed: 4994568]

Dworkin J, Losick R. Developmental commitment in a bacterium. Cell. 2005; 121:401–409. [PubMed: 15882622]

Errington J. Regulation of endospore formation in Bacillus subtilis. Nat Rev Microbiol. 2003; 1:117–126. [PubMed: 15035041]

Fleming TC, Shin JY, Lee SH, Becker E, Huang KC, Bustamante C, Pogliano K. Dynamic SpoIIIE assembly mediates septal membrane fission during Bacillus subtilis sporulation. Genes Dev. 2010; 24:1160–1172. [PubMed: 20516200]

Guerout-Fleury AM, Frandsen N, Stragier P. Plasmids for ectopic integration in Bacillus subtilis. Gene. 1996; 180:57–61. [PubMed: 8973347]

Gutierrez J, Smith R, Pogliano K. SpoIID-mediated peptidoglycan degradation is required throughout engulfment during Bacillus subtilis sporulation. J Bacteriol. 2010; 192:3174–3186. [PubMed: 20382772]

Jiang X, Rubio A, Chiba S, Pogliano K. Engulfment-regulated proteolysis of SpoIIQ: evidence that dual checkpoints control s^K activity. Mol Microbiol. 2005; 58:102–115. [PubMed: 16164552]

Levin PA, Fan N, Ricca E, Driks A, Losick R, Cutting S. An unusually small gene required for sporulation by Bacillus subtilis. Mol Microbiol. 1993; 9:761–771. [PubMed: 8231808]

Levin PA, Losick R. Transcription factor Spo0A switches the localization of the cell division protein FtsZ from a medial to a bipolar pattern in Bacillus subtilis. Genes Dev. 1996; 10:478–488. [PubMed: 8600030]

Liu NJ, Dutton RJ, Pogliano K. Evidence that the SpoIIIE DNA translocase participates in membrane fusion during cytokinesis and engulfment. Mol Microbiol. 2006; 59:1097–1113. [PubMed: 16430687]

Londono-Vallejo JA, Frehel C, Stragier P. SpoIIQ, a forespore-expressed gene required for engulfment in Bacillus subtilis. Mol Microbiol. 1997; 24:29–39. [PubMed: 9140963]

McKenney PT, Eichenberger P. Dynamics of spore coat morphogenesis in Bacillus subtilis. Mol Microbiol. 2012; 83:245–260. [PubMed: 22171814]

Meisner J, Wang X, Serrano M, Henriques AO, Moran CP Jr. A channel connecting the mother cell and forespore during bacterial endospore formation. Proc Natl Acad Sci U S A. 2008; 105:15100–15105. [PubMed: 18812514]

Meyer P, Gutierrez J, Pogliano K, Dworkin J. Cell wall synthesis is necessary for membrane dynamics during sporulation of Bacillus subtilis. Mol Microbiol. 2010; 76:956–970. [PubMed: 20444098]

Morlot C, Uehara T, Marquis KA, Bernhardt TG, Rudner DZ. A highly coordinated cell wall degradation machine governs spore morphogenesis in Bacillus subtilis. Genes Dev. 2010; 24:411–422. [PubMed: 20159959]

Perez AR, Abanes-De Mello A, Pogliano K. SpoIIB localizes to active sites of septal biogenesis and spatially regulates septal thinning during engulfment in *Bacillus subtilis*. J Bacteriol. 2000; 182:1096–1108. [PubMed: 10648537]

Piggot PJ, Hilbert DW. Sporulation of *Bacillus subtilis*. Curr Opin Microbiol. 2004; 7:579–586. [PubMed: 15556029]

Prajapati RS, Ogura T, Cutting SM. Structural and functional studies on an FtsH inhibitor from Bacillus subtilis. Biochim Biophys Acta. 2000; 1475:353–359. [PubMed: 10913836]

Ramamurthi KS, Clapham KR, Losick R. Peptide anchoring spore coat assembly to the outer forespore membrane in Bacillus subtilis. Mol Microbiol. 2006; 62:1547–1557. [PubMed: 17427285]

Ramamurthi KS, Lecuyer S, Stone HA, Losick R. Geometric cue for protein localization in a bacterium. Science. 2009; 323:1354–1357. [PubMed: 19265022]

Rodrigues CDA, Marquis KA, Meisner J, Rudner DZ. Peptidoglycan hydrolysis is required for assembly and activity of the transenvelope secretion complex during sporulation in *Bacillus subtilis*. Mol Microbiol. 2013

Rubio A, Pogliano K. Septal localization of forespore membrane proteins during engulfment in *Bacillus subtilis*. EMBO J. 2004; 23:1636–1646. [PubMed: 15044948]

Shapiro L, McAdams HH, Losick R. Why and how bacteria localize proteins. Science. 2009; 326:1225–1228. [PubMed: 19965466]

Sharp MD, Pogliano K. Role of cell-specific SpoIIIE assembly in polarity of DNA transfer. Science. 2002; 295:137–139. [PubMed: 11778051]

Sterlini JM, Mandelstam J. Commitment to sporulation in *Bacillus subtilis* and its relationship to development of actinomycin resistance. Biochem J. 1969; 113:29–37. [PubMed: 4185146]

Swan LE. Initiation of clathrin-mediated endocytosis: all you need is two? Bioessays. 2013; 35:425–429. [PubMed: 23440851]

Tocheva EI, Lopez-Garrido J, Hughes HV, Fredlund J, Kuru E, Vannieuwenhze MS, Brun YV, Pogliano K, Jensen GJ. Peptidoglycan transformations during *Bacillus subtilis* sporulation. Mol Microbiol. 2013; 88:673–686. [PubMed: 23531131]

van Ooij C, Losick R. Subcellular localization of a small sporulation protein in *Bacillus subtilis*. J Bacteriol. 2003; 185:1391–1398. [PubMed: 12562810]

Wu JQ, Sirotkin V, Kovar DR, Lord M, Beltzner CC, Kuhn JR, Pollard TD. Assembly of the cytokinetic contractile ring from a broad band of nodes in fission yeast. J Cell Biol. 2006; 174:391–402. [PubMed: 16864655]

Youngman P, Perkins JB, Losick R. A novel method for the rapid cloning in Escherichia coli of Bacillus subtilis chromosomal DNA adjacent to Tn917 insertions. Mol Gen Genet. 1984; 195:424–433. [PubMed: 6088944]

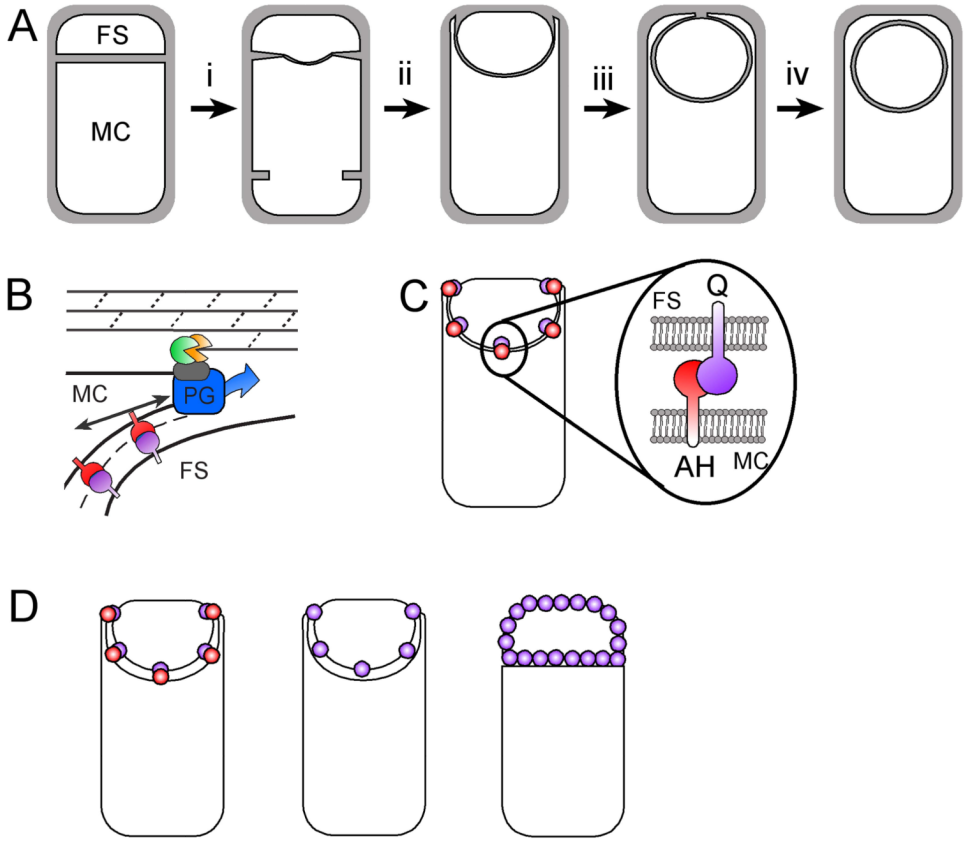

Figure 1. The process of engulfment during *Bacillus subtilis* sporulation

(A) The smaller forespore (FS) and larger mother cell (MC) initially lie side by side. Engulfment commences with septal thinning (i), during which septal peptidoglycan (light gray) is degraded. The mother cell membrane then migrates around the forespore (steps ii-iii), until it meets and fuses to release the forespore into the mother cell cytoplasm (step iv). (B) Engulfment in intact cells requires three mother cell membrane proteins, SpoIID (orange pacman), SpoIIM (oval), and SpoIIP (green pacman) that localize to the septum and leading edge of the engulfing membrane. SpoIID and SpoIIP degrade peptidoglycan, suggesting that engulfment might be mediated by the processive degradation of the peptidoglycan adjacent to the forespore membrane, which could move the mother cell membrane around the forespore. The SpoIIQ (purple) and SpoIIIAH (red) ratchet provides a backup mechanism for membrane migration (Broder & Pogliano, 2006). Membrane movement facilitated by peptidoglycan synthesis is indicated by the PG box and arrow, this machinery becomes required if SpoIIQ is deleted (Meyer et al., 2010). Figure adapted from (Meyer et al., 2010). (C) The zipper-like interaction between the forespore membrane protein SpoIIQ (labeled Q, purple) and the mother cell membrane protein SpoIIIAH (labeled AH, red) localizes SpoIIIAH (Blaylock et al., 2004, Doan et al., 2005), which recruits additional mother cell proteins (Doan et al., 2005, Blaylock et al., 2004). (D) Localization of SpoIIQ (purple circles) and SpoIIIAH (red circles) in wild type (wt), a *spoIIIAH* deletion (ΔAH), and σ^E deletion ($\Delta\sigma^E$).

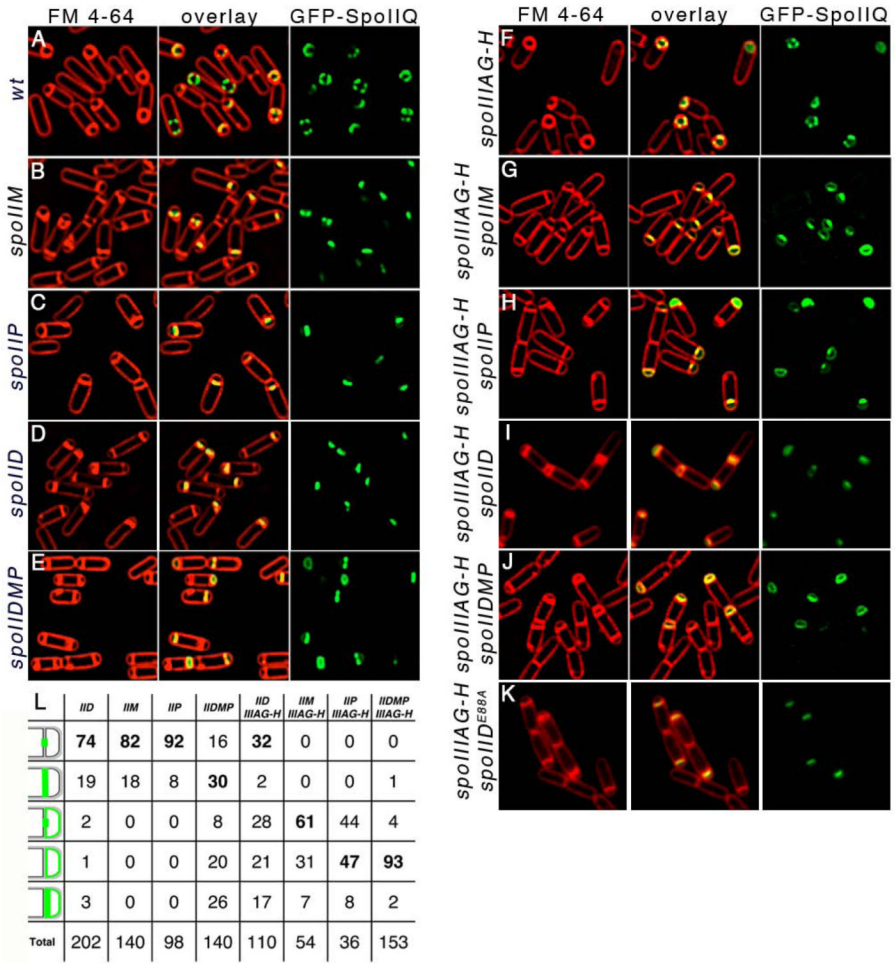

L	IID	IIM	IIP	IIDMP	IID IIIAG-H	IIM IIIAG-H	IIP IIIAG-H	IIDMP IIIAG-H
	74	**82**	**92**	16	**32**	0	0	0
	19	18	8	**30**	2	0	0	1
	2	0	0	8	28	**61**	44	4
	1	0	0	20	21	31	**47**	**93**
	3	0	0	26	17	7	8	2
Total	202	140	98	140	110	54	36	153

Figure 2. Localization of GFP-SpoIIQ in different mutant backgrounds

Samples were taken at $t_{2.5}$ after resuspension at 37°C and stained with FM 4-64 (red, left column) to visualize membranes. GFP images (green) are on the right with overlaid images in the middle. (A) Δ*spoIIQ*, *gfp-spoIIQ* (KP845) (*wt*), (B) *spoIIM-mls*, Δ*spoIIQ*, *gfp-spoIIQ* (AR140) (*spoIIM*), (C) *spoIIP::tet*, Δ*spoIIQ*, *gfp-spoIIQ* (KP848)(*spoIIP*), (D) *spoIID298*, *ΔspoIIQ*, *gfp-spoIIQ* (DB284)(*spoIID*), (E) *spoIID298*, *spoIIM-mls*, *spoIIP::tet*, Δ*spoIIQ*, *gfp-spoIIQ* (AR200) (*spoIIDMP*), (F) Δ*spoIIIAG-H-kan*, Δ*spoIIQ*, *gfp-spoIIQ* (KP872) (*spoIIIAGH*), (G) Δ*spoIIIAGH-kan*, *spoIIM-mls*, *ΔspoIIQ*, *gfp-spoIIQ* (DB150) (*spoIIIAGH spoIIM*), (H) Δ*spoIIIAGH-kan*, *spoIIP::tet*, *ΔspoIIQ*, *gfp-spoIIQ* (DB151)(*spoIIIAGH spoIIP*), (I) spoIID298, Δ*spoIIIAGH-erm*, *ΔspoIIQ*, *gfp-spoIIQ* (JFG526)(*spoIIIAGH spoIID*), (J) *spoIID298*, *spoIIM-mls*, *spoIIP::tet*, *ΔspoIIIAGH-kan*, *ΔspoIIQ*, *gfp-spoIIQ* (DB149) (*spoIIIAGH spoIIDMP*), (K) $spoIID^{E88A}$, Δ*spoIIIAGH-erm*, *ΔspoIIQ*, *gfp-spoIIQ* (JFG524)(*spoIIIAGH* $spoIID^{E88A}$); $spoIID^{E88A}$ cannot cleave peptidoglycan (L) $spoIID^{D210A}$, Δ*spoIIIAGH-erm*, *ΔspoIIQ*, *gfp-spoIIQ* (JFG520)(*spoIIIAGH* $spoIID^{D210A}$), (M) Summary of GFP-SpoIIQ localization in mutant backgrounds. For each localization pattern, numbers represent percent of total sporangia scored (bottom line) and may not add up to 100% due to rounding. Bold indicates category with highest percentage.

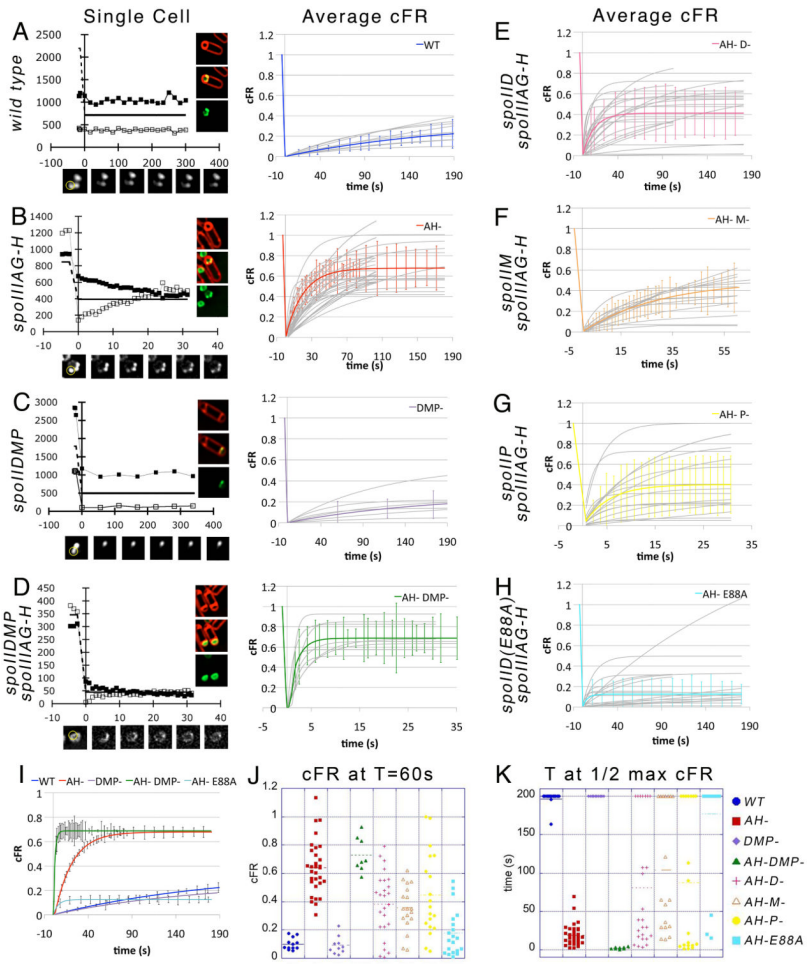

Figure 3. Photobleaching experiments demonstrate that immobility of GFP-SpoIIQ is primarily dependent on SpoIIIAH

(A-H) Strains expressing GFP-SpoIIQ (green) and carrying the indicated mutations were stained with FM 4-64 (red), applied to slides, and photobleached, imaged, quantified and plotted (see Experimental Procedures). The left column shows graphs and images of representative individual cells in color before photobleaching (on the right) and just GFP-SpoIIQ before and during recovery in black and white (below the graph), with bleached regions indicated by yellow circles. The graph shows the adjusted mean pixel intensity of the unbleached (black squares) and bleached (unfilled squares) regions and the theoretical pixel intensity value following equilibration between these regions (solid line). The right column of A-D and panels E-H show individual best fit, recovery curves (grey) for each cell. Curves were generated and normalized using the equations in (Wu et al., 2006), then averaged at each timepoint. The best fit of the averaged data is plotted to include standard deviation bars (colors). The corrected fraction recovery (cFR) is on the y-axis and time on the x-axis. A cFR of 0 represents no recovery and protein immobility, a cFR of 1 represents complete recovery in a cell with a large pool of unbleached GFP; the maximal cFR in our experiments averaged 0.7, since the forespore is small relative to the bleach spot.

Strains used: (A) Δ*spoIIQ::spc*, *gfp-spoIIQ* (KP845)(*wild type*), (B) Δ*spoIIQ::spc*, *gfp-spoIIQ*, *spoIIIAGH-kan* (KP872) (*spoIIIAG-H*), (C) Δ*spoIIQ::spc*, *gfp-spoIIQ*, *spoIID298*, *spoIIM-mls*, *ΔspoIIP::tet* (AR200) (*spoIIDMP*), (D) Δ*spoIIQ::spc*, *gfp-spoIIQ*, *spoIIIAGH-kan*, *spoIID298*, *spoIIM-mls*, *ΔspoIIP::tet* (DB149) (*spoIIDMP spoIIIAG-H*), (E) Δ*spoIIQ::spc*, *gfp-spoIIQ*, *spoIIIAGH-kan*, *spoIID298* (JFG526) (*spoIID spoIIIAG-H*), (F)

Δ*spoIIQ::spc*, *gfp-spoIIQ*, *spoIIIAGH-kan*, *spoIIM-mls* (DB150) (*spoIIM spoIIIAG-H*), (G) Δ*spoIIQ::spc*, *gfp-spoIIQ*, *spoIIIAGH-kan*, *ΔspoIIP::tet* (DB151) (*spoIIP spoIIIAG-H*), (H) $spoIID^{E88A}$, Δ*spoIIIAGH-erm*, *ΔspoIIQ*, *gfp-spoIIQ* (JFG524)(*spoIIIAGH* $spoIID^{E88A}$), (I) The average recovery curves with standard error for strains showing a clearly grouped single outcome. (J) Histogram showing the cFR for individual cells 60 seconds after photobleaching. A lower cFR represents decreased GFP-SpoIIQ mobility, and a cFR<0.2 was classified as immobile. (K) Histogram showing the time required for the cFR to reach 0.35, which is ½ of the average maximal recovery (0.7). $T_{1/2}$ >150 sec was considered immobile. Strains lacking any one of the engulfment proteins and SpoIIIAH show two recovery classes, fully immobile and intermediate to full mobility.

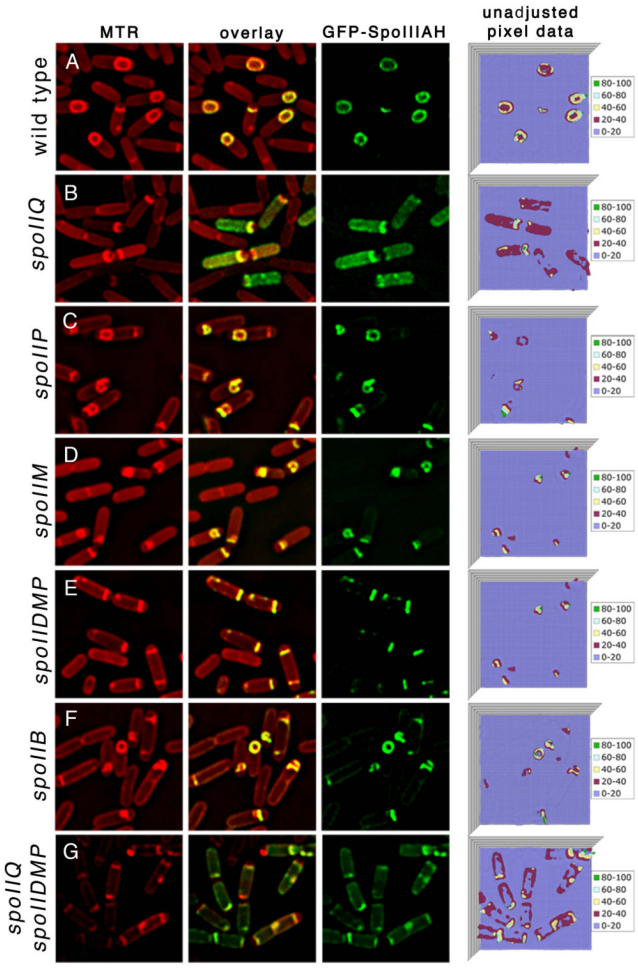

Figure 4. Localization of GFP-SpoIIIAH in different mutant backgrounds

Samples were taken at $t_{2.5}$ (A-F) after resuspension and stained with FM 4-64 (red, left column). GFP images (green) are on the right with overlaid images in the middle. (A) *gfp-spoIIIAH* (DB553), (B) Δ*spoIIQ::spc*, *gfp-spoIIIAH* (DB554), (C) Δ*spoIIP::tet*, *gfp-spoIIIAH* (DB555), (D) *spoIIM-mls*, *gfp-spoIIIAH* (DB556), (E) *spoIID298*, *spoIIM-mls*, *ΔspoIIP::tet*, *gfp-spoIIIAH* (DB557), (F) *spoIIB::erm*, *gfp-spoIIIAH* (DB558). The right column shows the pixel intensity data for the GFP.

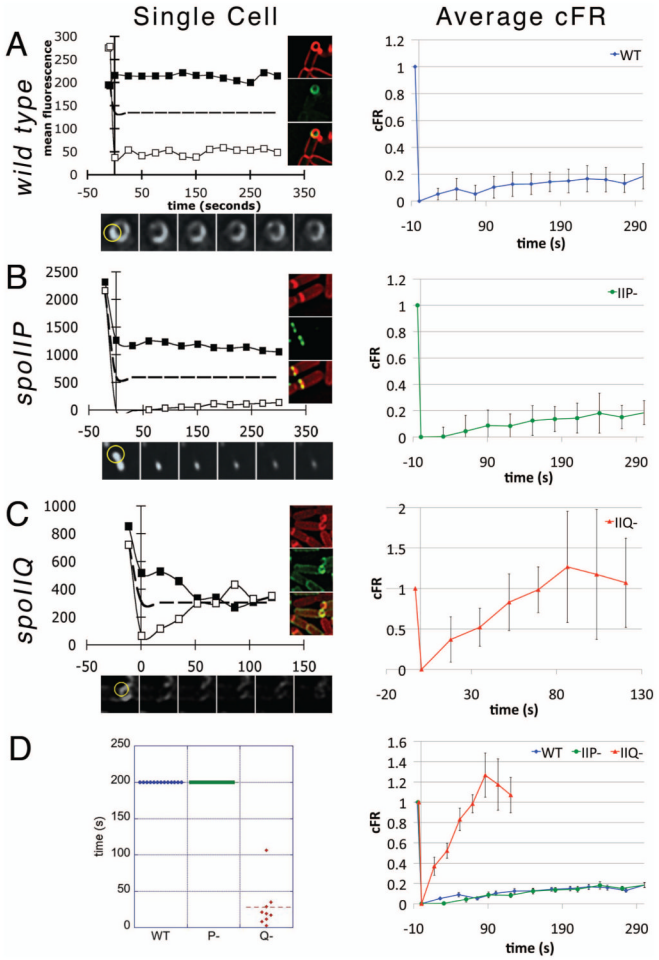

Figure 5. Immobility of GFP-SpoIIIAH is primarily dependent on SpoIIQ

Left column shows an example of one cell of each strain with black squares representing the unbleached region and white squares representing the bleached region. Right column shows the averaged corrected fraction recovery (cFR) with standard deviation bars. (A) *spoIIIAH, gfp-spoIIIAH* (DB542) (wild type), (B) Δ*spoIIP*, *spoIIIAH, gfp-spoIIIAH* (DB632) (*spoIIP)*, (C) Δ*spoIIQ*, *spoIIIAH, gfp-spoIIIAH* (DB631) (*spoIIQ)*, (D) Histogram showing the time required for the cFR to reach ½ of the maximal recovery. $T_{1/2}$ >150 sec was considered immobile and (left) comparison cFR graph with standard error bars.

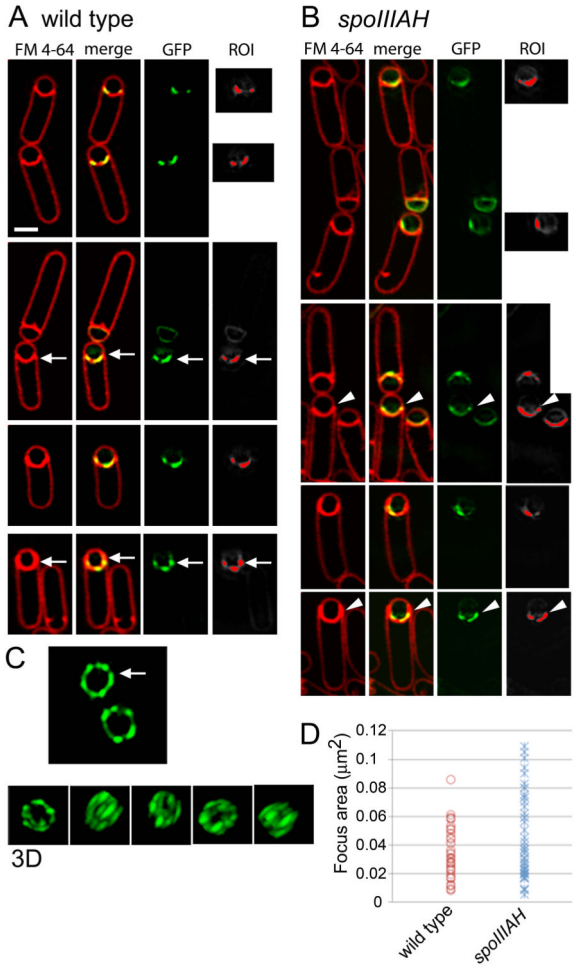

Figure 6. Super resolution imaging of GFP-SpoIIQ localization

(A-B) Sporulating cells expressing GFP-SpoIIQ (green) were harvested and stained with the fluorescent membrane stain FM 4-64 (red) and slides prepared as described. Imaging was performed on a structured illumination microscope (Applied Precision OMX), and the medial focal planes are shown. Foci were identified by using Image J to identify the brightest 60% of GFP-SpoIIQ fluorescence in each forespore, as shown in the region of interest (ROI) panels. This ROI was used to quantify the area and number of foci in the two strains (Table 1). (A) GFP-SpoIIQ shows more compact foci in the wild type strain, Δ*spoIIQ::spc*, *gfp-spoIIQ* (KP845), (arrows). (B) GFP-SpoIIQ shows more diffuse localization in a *spoIIIAH* background, Δ*spoIIQ::spc*, *gfp-spoIIQ*, *spoIIIAGH-kan* (KP872), (arrowheads). Scale bar = 1 μm. (C) 3D rotation of GFP-SpoIIQ in the wild type sporangium indicated by an arrow in the upper panel, which has completed engulfment. (D) Distribution of GFP-SpoIIQ foci area measured for *gfp-spoIIQ* (wild type) (circles) and *spoIIIAH*, *gfp-spoIIQ*(*spoIIIAH*) (asterisks). See also Table 1.

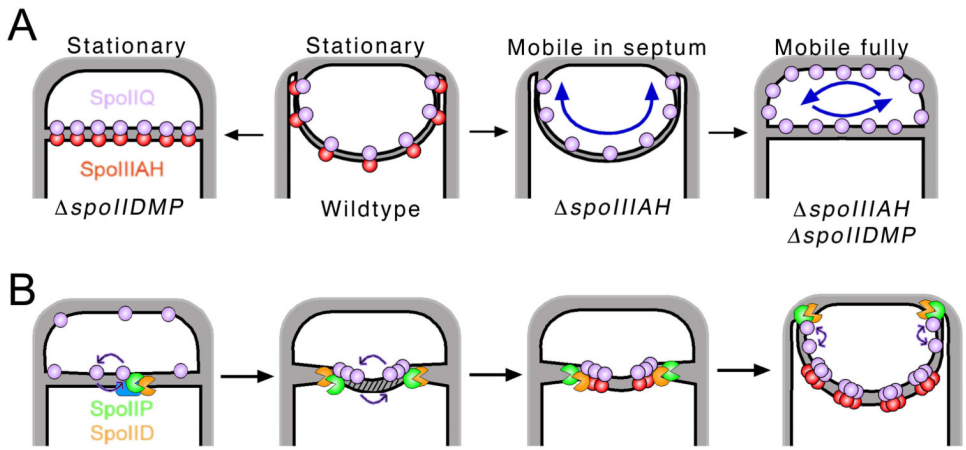

Figure 7. Model of SpoIIQ/SpoIIIAH/SpoIIDMP interactions

Cartoon depicting proposed interactions at the sporulation septum and SpoIIQ/SpoIIIAH localization. (A) When SpoIIIAH (red) is present, SpoIIQ (purple) localizes into a higher order structure independent of SpoIIDMP. When SpoIIIAH is missing, SpoIIQ organizes into a higher order structure across the septum and is highly mobile within that framework. When SpoIIIAH and SpoIIDMP are deleted, SpoIIQ is diffusely localized and freely mobile within the forespore membranes. (B) At the start of septal thinning, SpoIIQ (purple) transiently interacts with the SpoIID (orange), SpoIIP (green) and SpoIIM (blue) complex or their peptidoglycan cleavage products (indicated by black hatches over the grey peptidoglycan). A local concentration of SpoIIQ is created near the engulfment proteins, which localizes SpoIIIAH (red). SpoIIQ and SpoIIIAH form a complex behind the leading edges dictated by the concentration gradient, which forms continuously during engulfment.

Table 1

Size and number of GFP-SpoIIQ foci per cell observed using structured illumination microscopy

Strain	Avg. # of foci/cell[1]	St. dev.	Total cells	Avg. focus area[1] (μm²)	St. dev.	Total foci
wild type[2]	1.96	0.063	31	0.032	0.017	49
spoIIIAH[3]	1.55	0.068	25	0.044	0.029	48
	p=0.0018*			p=0.02*		

[1] Analysis of the number and area of foci in sporangia in which engulfment was less than 50% complete, as described in Experimental Procedures.

[2] Δ*spoIIQ*, *gfp-spoIIQ* (KP845)

[3] Δ*spoIIIAG-H-kan*, Δ*spoIIQ*, *gfp-spoIIQ* (KP872)

* p values were determined using an unpaired Student's t-test

Table 2

Strains used in this study

Strain	Genotype	Source
KP845	*ΔspoIIQ::spec, amyE::P_{spoIIQ}-GFP-spoIIQ-cm*	Rubio & Pogliano 2004
KP848	*ΔspoIIQ::spec, amyE:: P_{spoIIQ}-GFP-spoIIQ-cm, ΔspoIIP::tet*	Rubio & Pogliano 2004
KP849	*ΔspoIIQ::spec, amyE::P_{spoIIQ}-GFP-spoIIQ-cm, spoIIM-mls*	Rubio & Pogliano 2004
AR200	*ΔspoIIQ::spec, amyE:: P_{spoIIQ}-GFP-spoIIQ-cm, spoIID298, spoIIM-mls, ΔspoIIP::tet*	This work
DB149	*ΔspoIIQ::spec, amyE:: P_{spoIIQ}-GFP-spoIIQ-cm, spoIID298, spoIIM-mls, ΔspoIIP::tet, spoIIIAGH-kan*	This work
DB150	*ΔspoIIQ::spec, amyE::P_{spoIIQ}-GFP-spoIIQ-cm, ΔspoIIIAGH-kan, spoIIM-mls*	This work
DB151	*ΔspoIIQ::spec amyE::P_{spoIIQ}-GFP-spoIIQ-cm, ΔspoIIIAGH-kan ΔspoIIP::tet*	This work
DB153	*ΔspoIIQ::spec amyE:: P_{spoIIQ}-GFP-spoIIQ-cm ΔspoIIIAGH-kan, spoIID::cat::tet*	This work
KP4188	*spoIID298, spoIIM-mls, ΔspoIIP::tet*	This work
DB284	*ΔspoIIQ::spec, amyE:: P_{spoIIQ}-GFP-spoIIQ-cm, spoIID298*	This work
DB351	*spoIID298, spoIIM-mls, ΔspoIIP::tet, ΔspoIIIAGH-kan*	This work
DB542	*spoIIIAG::pMutinFLAG-erm, amyE::$P_{spoIIIA}$-GFP-spoIIIAH-cm*	This work
DB553	*amyE::$P_{spoIIIAA}$-GFP-spoIIIAH-cm*	This work
DB554	*amyE::$P_{spoIIIAA}$-GFP-spoIIIAH-cm, ΔspoIIQ::spec*	This work
DB555	*amyE::$P_{spoIIIAA}$-GFP-spoIIIAH-cm, ΔspoIIP::tet*	This work
DB556	*amyE::$P_{spoIIIAA}$-GFP-spoIIIAH-cm, spoIIM-mls*	This work
DB557	*amyE::$P_{spoIIIAA}$-GFP-spoIIIAH-cm, spoIID298, spoIIM-mls, ΔspoIIP::tet*	This work
DB558	*amyE::$P_{spoIIIAA}$-GFP-spoIIIAH-cm, spoIIB::erm*	This work
DB631	*spoIIIAG::pMutinFLAG-erm, amyE::$P_{spoIIIAA}$-GFP-spoIIIAH-cm, ΔspoIIQ::spec*	This work
DB632	*spoIIIAG::pMutinFLAG-erm, amyE::$P_{spoIIIAA}$-GFP-spoIIIAH-cm, ΔspoIIP::tet*	This work
KP896	*ΔspoIIIAGH-kan*	(Blaylock et al., 2004)
KP872	*ΔspoIIQ::spec, amyE:: P_{spoIIQ}-GFP-spoIIQ-cm, spoIIIAGH-kan*	(Blaylock et al., 2004)
JFG510	*ΔspoIIQ::spec; amyE:: P_{spoIIQ}-GFP-spoIIQ-cm; spoIID298; thrC::P_{spoIID}-spoIID^{E88A}-kan*	This work
JFG513	*ΔspoIIQ::spec; amyE:: P_{spoIIQ}-GFP-spoIIQ-cm; spoIID298; thrC::P_{spoIID}-spoIID^{D210A}-kan*	This work
JFG514	*ΔspoIIQ::spec; amyE:: P_{spoIIQ}-GFP-spoIIQ-cm; spoIID298; thrC::P_{spoIID}-spoIID-kan*	This work
JFG520	*ΔspoIIQ::spec; amyE:: P_{spoIIQ}-GFP-spoIIQ-cm; spoIID298; thrC::P_{spoIID}-spoIID^{D210A}-kan; spoIIIAG::pMutinFLAG-erm*	This work
JFG522	*ΔspoIIQ::spec; amyE:: P_{spoIIQ}-GFP-spoIIQ-cm; spoIID298; thrC::P_{spoIID}-spoIID-kan; spoIIIAG::pMutinFLAG-erm*	This work
JFG524	*ΔspoIIQ::spec; amyE:: P_{spoIIQ}-GFP-spoIIQ-cm; spoIID298; thrC::P_{spoIID}-spoIID^{E88A}-kan; spoIIIAG::pMutinFLAG-erm*	This work
JFG526	*ΔspoIIQ::spec; amyE:: P_{spoIIQ}-GFP-spoIIQ-cm; spoIID298; spoIIIAG::pMutinFLAG-erm*	This work
pDB102	*spoIIIAG::pMutinFLAG-erm (spoIIIAH-)*	This work
pDB142	*$P_{spoIIIAA}$-GFP-spoIIIAH-Cm*	This work
pJFG77	*thrC::P_{spoIID}-spoIID-kan*	This work

Strain	Genotype	Source
pJFG78	*thrC::*P_{spoIID}*-spoIID*^{D210A}*-kan*	This work
pJFG79	*thrC::*P_{spoIID}*-spoIID*^{E88A}*-kan*	This work